Resonance Raman Spectroscopic Study of Nitrophorin 1, a Nitric Oxide-Binding Heme Protein from *Rhodnius prolixus*, and Its Nitrosyl and Cyano Adducts

Estelle M. Maes,[†] F. Ann Walker,[‡] William R. Montfort,[‡] and Roman S. Czernuszewicz*[,†]

Contribution from the Department of Chemistry, University of Houston, Houston, Texas 77204, and Departments of Chemistry and Biochemistry, University of Arizona, Tucson, Arizona 85721

Received August 28, 2000. Revised Manuscript Received June 29, 2001

Abstract: The resonance Raman (RR) spectra of nitrophorin 1 (NP1) from the saliva of the blood-sucking insect *Rhodnius prolixus*, in the absence and presence of nitric oxide (NO) and in the presence of cyanide (CN^-), have been studied. The NP1 displayed RR spectra characteristic of six-coordinate high-spin (6cHS) ferric heme at room temperature and six-coordinate low-spin heme (6cLS) at low temperature (77 K). NO and CN^- each bind to Fe^{III}, both ligands forming 6cLS complexes with NP1. The $Fe^{III}-NO$ stretching and bending vibrational frequencies of nitrosyl NP1 were identified at 591 and 578 cm^{-1}, respectively, on the basis of ^{15}NO isotope shifts. These frequencies are typical of Fe−NO ferric heme proteins, indicating that the NP1 nitrosyl adduct has typical bond strength. Thus, the small NO release rate displayed by NP1 must be due to other protein interactions. Room and cryogenic temperature (77 K) RR spectroscopy and ^{13}C, ^{15}N, and $^{13}C^{15}N$ isotope substitutions have been used to determine vibrational mode frequencies associated with the $Fe^{III}-CN^-$ bond for the cyano adducts at 454, 443, 397, and 357 cm^{-1}. The results were analyzed by normal mode calculations to support the assignment of the modes and to assess the NO and CN^- binding geometries. The observed isotope shifts for the cyano NP1 are smaller than expected and reveal vibrational coupling of $Fe^{III}-CN^-$ modes with heme modes. We also find that the observed frequencies are consistent with the presence of a nearly linear $Fe^{III}CN^-$ linkage (173°) coexisting with a population with a bent structure (155°).

Introduction

Blood-sucking insects contain a large array of salivary substances that act as antihemostatic factors, including anticoagulants, antiplatelet aggregation agents, and vasodilators, to overcome their hosts' defense against blood loss.[1−4] *Rhodnius prolixus*, a member of the Kissing bug family from South America, has four vasodilatory proteins that facilitate blood flow to the site of the wound and interfere with blood clotting and inflammation.[5,6] These proteins, named "nitrophorins", are ferric heme proteins that are reversible carriers of nitric oxide (NO) and tight binders of histamine.[7] Nitrophorins were the first proteins shown to have the capacity for NO storage in one tissue (the bug's salivary glands) and NO release in another (the host's skin) due to a pH-dependent NO binding affinity.[4,6,8,9] The small toxic gaseous NO molecule, released due to dilution and pH elevation upon injection of the nitrophorins into the victim, diffuses from the wound site through the tissue to the capillaries and causes vasodilation. Studies at different pH values reveal that the degree of NO binding, the rate of NO release, and the Soret absorption maxima for nitrophorins are pH dependent.[6,9,10]

Recently, the genes for all four nitrophorins of *R. prolixus*, referred to as NP1−NP4, have been cloned, expressed, and functionally characterized,[9−12] and the crystal structures of NP1, NP2, and NP4 determined.[12−14] Release of NO was found to be multiphasic in all four proteins, indicating that a complicated release mechanism was at work. The hemes in the proteins were all found to be highly distorted, adopting predominately ruffled conformations. The crystal structure of ferric NP4(NO) revealed an extensive conformational change on binding NO that resulted in desolvation of the protein's distal pocket and the packing of nonpolar amino acids next to the NO. The NO moiety was found to occupy multiple orientations in this structure, possibly due to photodissociation or partial reduction of the heme iron by

* Author to whom correspondence should be addressed: (fax) (713)-743-2709; (e-mail) Roman@uh.edu.
† University of Houston.
‡ University of Arizona.

(1) Ribeiro, J. M. C.; Garcia, E. S. *J. Exp. Biol.* **1981**, *94*, 219−230.
(2) Ribeiro, J. M. C.; Rossignol, P. A.; Spielman, A. *J. Exp. Biol.* **1984**, *108*, 1−7.
(3) Ribeiro, J. M. C. *Annu. Rev. Entomol.* **1987**, *32*, 463−478.
(4) Law, J.; Ribeiro, J. M. C.; Wells, M. A. *Annu. Rev. Biochem.* **1992**, *61*, 87−111.
(5) Ribeiro, J. M. C.; Gonzales, R.; Marinotti, O. *Br. J. Pharmacol.* **1990**, *101*, 932−936.
(6) Ribeiro, J. M. C.; Hazzard, J. M. H.; Nussenzveig, R. H.; Champagne, D. E.; Walker, F. A. *Science* **1993**, *260*, 539−541.
(7) Champagne, D. E.; Nussenzveig, R. H.; Ribeiro, J. M. C. *J. Biol. Chem.* **1995**, *270*, 8691−8695.
(8) Valenzuela, J. G.; Walker, F. A.; Ribeiro, J. M. C. *J. Exp. Biol.* **1995**, *198*, 1519−1526.
(9) Andersen, J. F.; Champagne, D. E.; Weichsel, A.; Ribeiro, J. M. C.; Balfour, C. A.; Dress, V.; Montfort, W. R. *Biochemistry* **1997**, *36*, 4423−4428.
(10) Andersen, J. F.; Ding, X. D.; Balfour, C.; Shokhireva, T. K.; Champagne, D. E.; Walker, F. A.; Montfort, W. R. *Biochemistry* **2000**, *39*, 10118−10131.
(11) Ding, X. D.; Weichsel, A.; Andersen, J. F.; Shokhireva, T. K.; Balfour, C.; Pierik, A. J.; Averill, B. A.; Montfort, W. R.; Walker, F. A. *J. Am. Chem. Soc.* **1999**, *121*, 128−138.
(12) Andersen, J. F.; Weichsel, A.; Balfour, C. A.; Champagne, D. E.; Montfort, W. R. *Structure* **1998**, *6*, 1315−1327.
(13) Weichsel, A.; Andersen, J. F.; Champagne, D. E.; Walker, F. A.; Montfort, W. R. *Nature Struct. Biol.* **1998**, *5*, 304−309.
(14) Andersen, J. F.; Montfort, W. R. *J. Biol. Chem.* **2000**, *275*, 30496−30503.

10.1021/ja0031927 CCC: $20.00
Published on Web 11/02/2001

the X-ray beam ($\lambda = 1.54$ Å).[15] A second NP4(NO) structure, measured with higher energy X-rays ($\lambda = 0.975$ Å) and determined to very high resolution (1.08 Å), displayed a single NO conformation with a bond length of 1.66(1) Å and bond angle of 156(1)°.[16] Both this structure and the cyano NP4 complex (bond length = 1.96 Å, bond angle = 158°) displayed a substantial increase in heme distortion with respect to the aqua complex, apparently due to π orbital donation by the ligands. Only binding of NO, however, led to a conformational change in the protein. The structure of the NP1 cyano complex has also been determined, but only to a resolution of 2.3 Å, leading to a less precise model with an Fe−C−N bond angle of approximately 173°.[13] The crystal structure of ferric NP1(NO) has not yet been determined.

The present study focuses on the vibrational spectroscopy of the nitrosyl and cyano complexes of NP1 to further clarify the ligand geometry in the nitrophorins. NP1 is the most abundant of the *Rhodnius* nitrophorins, was the first available in high quantity,[9] and is the most thoroughly characterized.[11] The NP1 amino acid sequence is 90%, identical with that of NP4, and its kinetic parameters are also quite similar, suggesting that no major differences exist between the two proteins. In contrast, NP2 and NP3 display altered kinetics, lower sequence homology, and key structural differences with NP1 and NP4.[10,14]

Of the spectroscopic methods available for characterization of heme protein active sites, resonance Raman (RR) spectroscopy is a particularly powerful technique because excitation within the heme $\pi-\pi^*$ electronic absorption transitions selectively enhances vibrational modes of the heme and bound ligands without interference from the modes associated with the protein matrix.[17] Herein, we describe the main features of the nitrophorin RR scattering by analyzing the Soret-excitation spectra of *R. prolixus* NP1 at room and low temperatures. We also present the results of RR study of the complex of NP1 with nitric oxide, NP1(NO). NO is involved in important biological activities such as blood pressure regulation, neurotransmission, cell mediated immune response, muscle relaxation, vasodilation, prevention of platelet aggregation,[18,19] and activation of enzymes such as guanylyl cyclase.[20] NO binds to ferrous heme proteins with very high affinity but, unlike CO, also binds reasonably well to ferric hemes. RR spectroscopy has proven to be the most effective tool for observing Fe−ligand vibrational modes whose frequencies reflect the strength of ligand binding, the ligand disposition, and the ligand−protein interactions.[21,22] Of particular interest in this regard is whether the slow rate of NO release exhibited by the nitrophorins is due to a stronger Fe−NO bond or to some other factor such as the closed protein conformation that occurs in the nitrosyl complex. In this study, we provide structural information regarding the NP1−nitric oxide interaction by searching for a characteristic vibrational frequency associated with the Fe^{II}−NO bond in the RR spectrum of NP1(NO). We also examine the heme conformation by analyzing the sensitivity of NP1 skeletal vibrational modes to NO binding. In addition, the RR spectra of NP1 ligated to cyanide anion, NP1(CN^-), were recorded to characterize the effect of this exogenous ligand on the heme pocket and to further monitor the subtle structural changes caused by different heme distal environments.

Experimental Section

Sample Preparation. Recombinant NP1 expression, isolation, and purification were carried out as described earlier.[9] After being eluted from a cation exchange column (pH 5.0) and dialyzed against several changes of water, the protein was then lyophilized. Solutions were prepared by dissolving the lyophilized protein in the appropriate buffer (sodium phosphate, pH 7.0, or sodium acetate, pH 5.0).

NO-bound NP1 was prepared in the following way: approximately 300 μL of a 0.3 mM NP1 solution was transferred into a 5-mm-diameter NMR tube sealed with a rubber septum. The atmospheric oxygen in the solution was removed by repeated evacuation and flushing with oxygen-free argon (argon was passed through an Oxy-purge cartridge purchased from Alltech). NO (purchased from Matheson), cleaned by passage through a column of potassium hydroxide solution (0.5 M), was introduced to the NMR tube via a line purged with argon. The formation of the NP1(NO) complex resulted in a change of color of the protein solution from light brown to dark pink. The NP1(^{15}NO) derivative was made by in situ generation of ^{15}NO from 100 mg of solid $Na^{15}NO_2$ (enrichment >98%, obtained from Cambridge Isotope Laboratories) and 15 mL of anaerobic 0.2 M KI/0.4 M H_2SO_4.[11] The NMR tube containing the protein solution was placed in series with a sealed vial where the reduction of $NaNO_2$ occurred. The preparation of NP1(^{15}NO) was performed by applying pressure in the sealed vial, allowing ^{15}NO to be introduced into the NMR tube and bind to the protein.

The cyano complexes were formed by addition of approximately 5-fold excess of KCN (100 mM phosphate buffer, pH 7.0). The addition of KCN resulted in a change in the protein solution color to cherry red. The isotopically labeled cyanides ($K^{13}C^{14}N$, $K^{12}C^{15}N$, and $K^{13}C^{15}N$ at 99% enrichment) were a generous gift from Dr. James R. Kincaid, Marquette University.

Resonance Raman Spectroscopy. RR spectra were recorded under the control of a Spex DM3000 microcomputer system using a conventional scanning Raman instrument equipped with a Spex 1403 double monochromator (with a pair of 1800 grooves/mm gratings) and a Hamamatsu 928 photomultiplier detector.[23,24] The excitation line (413.1 nm) was provided by a Coherent K-2 Kr^+ ion laser. For measurements at room temperature, the sample contained in an NMR tube was positioned in a backscattering geometry and kept spinning to prevent photodissociation and to avoid local thermal degradation of the protein during the spectral acquisition process. Details of this sampling technique are presented elsewhere.[25] Under this condition no protein damage was observed, even during prolonged spectral data acquisition. To accurately determine isotope shifts, the monochromator position was carefully calibrated against Rayleigh scattering and samples with different isotopes were recorded the same day. For measurements at low temperature (77 K), backscattered photons were collected directly from the surface of a frozen protein solution held in a vacuum on a coldfinger of a liquid nitrogen cryostat.[23,26] To ensure accurate determination of isotope shifts, natural abundance and isotopically labeled samples were affixed in pairs on the coldfinger so that RR spectra were recorded under identical conditions. The monochromator was advanced in 0.5- or 0.2-cm^{-1} increments in the case of isotope measurements and integration times were 1 s per data point. Improvements in the signal-to-noise ratio were achieved by averaging multiple

(15) Weichsel, A.; Andersen, J. F.; Roberts, S. A.; Montfort, W. R. *Nature Struct. Biol.* **2000**, *7*, 551−554.
(16) Roberts, S. A.; Weichsel, A.; Montfort, W. R. To be submitted for publication.
(17) Kincaid, J. R. In *The Porphyrin Handbook*; Kadish, K. M., Smith, K. M., Guilard, R., Eds.; Academic Press: San Diego, 2000; Vol. 7, pp 225−291.
(18) Bredt, D. S.; Snyder, S. H. *Annu. Rev. Biochem.* **1994**, *63*, 175−195.
(19) Schmidt, H. H. H. W.; Walter, U. *Cell* **1994**, *78*, 919−925.
(20) Zhao, Y.; Hogangson, C.; Babcock, G. T.; Marletta, M. A. *Biochemistry* **1998**, *37*, 12458−12464.
(21) *Biological Applications of Raman Spectroscopy*; Spiro, T. G., Ed.; Wiley-Interscience: New York, 1988; Vol. 3.
(22) Yu, N.-T. *Methods Enzymol.* **1986**, *130*, 350−409.
(23) Czernuszewicz, R. S. In *Methods in Molecular Biology*; Jones, C., Muloy, B., Thomas, A. H., Eds.; Humana Press: Totowa, NJ, 1993; Vol. 17, pp 345−374.
(24) Spiro, T. G.; Czernuszewicz, R. S. *Methods Enzymol.* **1995**, *246*, 416−460.
(25) Walters, M. A. *Appl. Spectrosc.* **1983**, *37*, 299−301.
(26) Czernuszewicz, R. S.; Johnson, M. K. *Appl. Spectrosc.* **1983**, *37*, 297−298.

scans (2−14). The slowly sloping baselines in the range 1100−1700 cm^{-1} were subtracted from the digitally collected spectra by using a LabCalc software package (Galactic Industries, Inc.). No baseline corrections were applied to the low-frequency spectra (200−800 cm^{-1}). For the 295−465 cm^{-1} spectral region of frozen NP1 and its cyano isotopomers, a LabCalc CURVEFIT routine was used to deconvolute overlapped peaks into a combination of Gaussian curves. Initial number, positions, and bandwidths of NP1(CN^-) peaks were obtained from curve fitting analysis of the NP1 spectrum. So far as possible, an identical bandwidth was used for corresponding peaks of isotopomers. IGOR Pro (Version 3.12) software (WaveMetrics, Inc.) was used to prepare the spectral figures.

Normal-Mode Analysis. Normal-mode calculations were performed by the Wilson **GF** matrix method with use of a general valence force field.[27] All calculations were carried out on a Silicon Graphics INDY workstation with a UNIX version of the RAMVIB software package[28] to construct the **G** and **F** matrices and to solve the secular equations. A simplified eight-atom model was used, in which the porphyrin system was represented by four nitrogen atoms (N_p) with equal mass (108 amu) and equally distant from the iron atom. For histidine, the imidazole (Im) was considered perpendicular to the porphyrin ring and treated as a point mass of 68 amu. The Fe−C−N angle formed by the cyanide ligand was first set to 173° to model the geometry of the cyano NP1 structure determined by X-ray crystallography.[13] In the absence of crystal structure data for NP1($Fe^{III}NO$), the Fe−N−O angle was also initially set to 173°. The following bond lengths (Å) were used: (Im)N−Fe = 2.052, Fe−N_p = 1.981, Fe−C_{CN} = 1.879, C−N = 1.148, Fe−N_{NO} = 1.740, and N−O = 1.100.[13,29] Initial values of force constants were estimated from previously calculated force fields.[29−31]

Results and Discussion

NP1. RR spectra of metalloporphyrins excited near resonance with the Soret absorption band are dominated by totally symmetric (A_{1g} for a D_{4h} metalloporphyrin) in-plane stretching modes of the porphyrin ring: ν_2 (∼1570 cm^{-1}), ν_3 (∼1490 cm^{-1}), and ν_4 (∼1370 cm^{-1}).[32,33] The high-frequency RR spectra of the heme proteins are known to contain a number of characteristic marker bands that are sensitive to the oxidation state and also to the coordination and spin state of the central iron atom.[17,21,22] Figure 1 displays the 1075−1675-cm^{-1} region of the RR spectra of *R. prolixus* NP1 obtained at (a) 298 and (b) 77 K with Soret band (413.1 nm) excitation. The oxidation state marker band ν_4 is observed at 1372 and 1376 cm^{-1} at 298 and 77 K, respectively, frequencies that are characteristic of ferric heme proteins. As expected, a decrease in temperature causes an overall upshift by ∼3−6 cm^{-1} of the RR marker bands due to an increase of protein packing forces.[34] The ν_3 porphyrin skeletal mode is well established to be sensitive to the heme core size which changes with the spin state of the iron. Typically, ν_3 has distinct frequencies for six-coordinate low-spin (6cLS) (1500−1510 cm^{-1}), five-coordinate high-spin (5cHS) (1490−1500 cm^{-1}), and six-coordinate high-spin (6cHS) (1475−1485 cm^{-1}) hemes.[35] At 298 K, the ν_3 mode of NP1 at 1481 cm^{-1} reveals the presence of a 6cHS nitrophorin population. At 77 K, the ν_3 mode is upshifted to 1509 cm^{-1}, which indicates the formation of a 6cLS population. The spectral pattern in the high-frequency region of NP1 at room temperature resembles very closely that of ferric myoglobin (metMb) at pH 7.0 in terms of relative band intensities and frequencies[36] and assignments of the RR bands of NP1 are adapted from those reported for metMb by Hu et al.[36] (Table 1). The other structure-sensitive modes, ν_2 and ν_{10} (Table 1), are also consistent with the assignments of 6cHS and 6cLS populations at room and low temperatures, respectively.[34] The observation of weaker bands at 1512 (ν_3) and 1582 cm^{-1} (ν_2) in the spectrum at 298 K could suggest the presence of a minor 6cLS population in NP1 at room temperature. However, these bands coincide with bands due to other porphyrin skeletal modes, ν_{38} and ν_{37}, respectively.[36] Moreover, the near absence of ν_{10} at ∼1640 cm^{-1} that is characteristic of the 6cLS population confirms that the heme in NP1 exists mainly as a 6cHS species at room temperature.

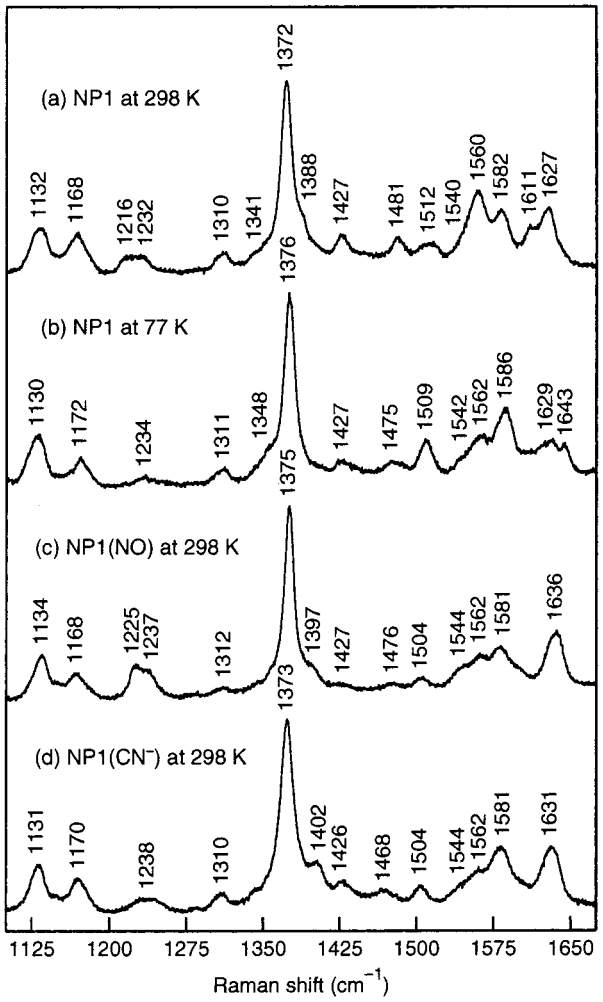

Figure 1. High-frequency (1075−1675 cm^{-1}) RR spectra of NP1 at (a) 298 and (b) 77 K and of (c) nitrosyl and (d) cyano NP1 at 298 K. Spectra were obtained via backscattering from a spinning NMR tube (298 K)[25] or from the surface of a frozen protein solution kept in a liquid-N_2 dewar (77 K):[26] 413.1-nm excitation, 70- (298 K) and 150-mW (77 K) laser power, 6-cm^{-1} slit widths.

(27) Wilson, E. B.; Decius, J. C.; Gross, P. C. *Molecular Vibrations*; McGraw-Hill: New York, 1955.
(28) Fraczkiewicz, R.; Czernuszewicz, R. S. *J. Mol. Struct.* **1997**, *435*, 109−121.
(29) Hu, S.; Kincaid, J. R. *J. Am. Chem. Soc.* **1991**, *113*, 2843−2850.
(30) López-Garriga, J. J.; Oertling, W. A.; Kean, R. T.; Hoogland, H.; Wever, R.; Babcock, G. T. *Biochemistry* **1990**, *29*, 9387−9395.
(31) Simianu, M. C.; Kincaid, J. R. *J. Am. Chem. Soc.* **1995**, *117*, 4628−4636.
(32) Spiro, T. G.; Czernuszewicz, R. S.; Li, X.-Y. *Coord. Chem. Rev.* **1990**, *100*, 541−571.
(33) Czernuszewicz, R. S.; Maes, E. M.; Rankin, J. G. In *The Porphyrin Handbook*; Kadish, K. M., Smith, K. M., Guilard, R., Eds.; Academic Press: San Diego, 2000; Vol. 7, pp 293−337.
(34) Feis, A.; Marzocchi, M. P.; Paoli, M.; Smulevich, G. *Biochemistry* **1994**, *33*, 4577−4583.
(35) Spiro, T. G.; Stong, J. D.; Stein, P. *J. Am. Chem. Soc.* **1979**, *101*, 2648−2655.
(36) Hu, S.; Smith, K. M.; Spiro, T. G. *J. Am. Chem. Soc.* **1996**, *118*, 12638−12646.

Table 1. Resonance Raman High Frequencies (cm^{-1}) and Their Mode Assignments for Nitrophorin 1 (NP1) and MetMyoglobin (metMb)

mode	NP1[a] 77 K	NP1[a] 298 K	metMb[b] 298 K
$\nu(C_aC_b)_{vinyl}$	1629	1627	1621
ν_{10}, $\nu(C_\alpha C_m)_{asym}$	1643	1611	1608
ν_{37}, $\nu(C_\alpha C_m)_{asym}$	1586[c]	1582	1583
ν_2, $\nu(C_\beta C_\beta)$	1586[c]	1560	1563
ν_{11}, $\nu(C_\beta C_\beta)$	1562	1540	1544
ν_{38}, $\nu(C_\beta C_\beta)$	1542	1512	1511
ν_3, $\nu(C_\alpha C_m)_{sym}$	1509	1481	1483
$\delta(C_bH_2)_{sym,\ vinyl}$	1475		1451
ν_{28}, $\nu(C_\alpha C_m)_{sym}$	1427	1427	142
ν_{12}, ν(Pyr. half-ring)$_{sym}$		1388	1389
ν_4, ν(Pyr. half-ring)$_{sym}$	1376	1372	1373
ν_{41}, ν(Pyr. half-ring)$_{sym}$	1348	1341	1341
$\delta(C_aH)_{vinyl}$	1311	1310	1316
	1234	1232	1223
ν_{13}, $\delta(C_mH)$		1216	1209
ν_{30}, ν(Pyr. half-ring)$_{asym}$	1172	1168	1169
ν_{14}, $\nu(C_\beta C_1)_{sym}$	1130	1132	1135

[a] This work. [b] Data and assignment from Hu et al.[36] [c] Overlapping bands.

The low-frequency heme RR spectra contain in-plane and out-of-plane heme deformation modes that are sensitive to heme peripheral substituent orientation and features that are associated with bound axial ligands. Figure 2a shows the RR spectrum of NP1 in the 200−800-cm^{-1} region obtained at 298 K. The heme of NP1 is ligated to a histidine residue as its proximal ligand, just as in metMb. However, RR studies of heme proteins and model compounds have shown that the $\nu(Fe-N_{His})$ stretching vibration is only observable for five-coordinate ferrous hemes.[37] The pattern of the spectrum of NP1 in the low-frequency region is quite different from that of metMb, in particular in the number of bands in the 400−450-cm^{-1} region and the relative intensity of the 376-cm^{-1} band.[36] Recent RR studies of metMb provided a very detailed set of assignments for low-frequency modes of protohemin IX (Table 2).[36] The 400−450-cm^{-1} region contains in-plane bending modes of the two vinyl substituents. The 376-cm^{-1} band, which is the strongest band below 600 cm^{-1} for metMb, has been attributed to a mode involving porphyrin−propionate bending and its intensity variation may be related to conformational changes of the propionate substituents. The differences in RR spectrum observed between NP1 and metMb appear to reveal differences in the conformation of peripheral substituents. In fact, the low-frequency region of the NP1 RR spectrum resembles more that of the heme−heme oxygenase (HO) complex (isoform 1), which has the same axial ligands as metMb, in terms of the number of bands and relative intensities.[38] The differences in the low RR frequencies between heme−HO and metMb have been attributed to differences in their heme pocket allowing a greater amount of freedom of the peripheral substituents in the heme−HO complex.

Nitric Oxide Binding to NP1. In contrast to other heme proteins whose ferric nitrosyl complexes undergo autoreduction,[39] the ferric NO complex of NP1, NP1(NO), is quite stable under anaerobic conditions and no change is detected in the RR spectrum over several weeks, indicating no autoreduction

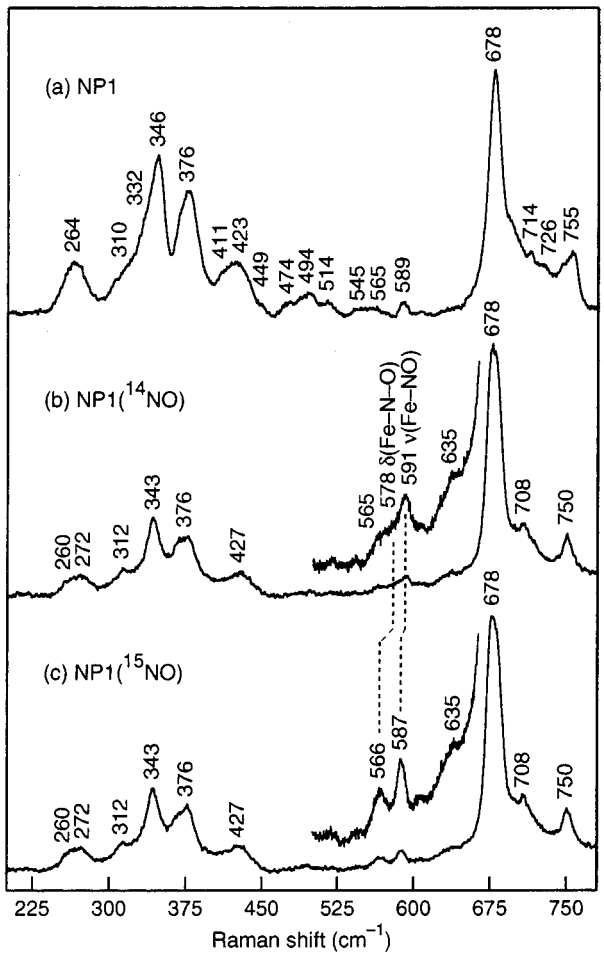

Figure 2. Low-frequency (200−800 cm^{-1}) RR spectra of (a) NP1 and its nitrosyl adduct in (b) natural abundance and (c) ^{15}NO-labeled obtained from spinning NMR tubes at room temperature: 413.1-nm excitation, 70-mW for NP1, 30-mW for NP1(NO), 6-cm^{-1} slit widths.

Table 2. Resonance Raman Low Frequencies (cm^{-1}) and Their Mode Assignments for Nitrophorin 1 (NP1), Heme−Heme Oxygenase (HO) Complex (isoform 1), and metMyoglobin (metMb)

mode	NP1[a] 77 K	NP1[a] 298 K	heme−HO[b] 298 K	metMb[c] 298 K
ν_{15}, ν(Pyr. breathing)	749	755	758	757
γ_5, Pyr. fold$_{sym}$		726		721
γ_{11}, Pyr. fold$_{asym}$	715	714	715	715
ν_7, δ(Pyr. deform.)$_{sym}$	677	678	677	674
ν_{48}, δ(Pyr. deform.)$_{sym}$	589	589	587	584
	565	565		
γ_{21}, Pyr. fold$_{sym}$	545	545	553	547
	514	514		
γ_{12}, Pyr. swivel	493	494	504	502
ν_{33}, δ(Pyr. rot.)	470	474		475
$\delta(C_\beta C_aC_b)_2 + \delta(C_\beta Me)$	449	449		440
	433			
	423	423	423	
$\delta(C_\beta C_aC_b)_4 + \delta(C_\beta Me)$	412	411	411	409
$\delta(C_\beta C_cC_d)$	376	376	379	376
ν_8, $\nu(FeN_p)$	348	346	346	344
γ_6, Pyr. tilt.		332		337
γ_7, $\gamma(C_\alpha C_m)$	313	310		305
ν_{52}, $\gamma(C_\alpha C_m)$	268	264[d]	262	271
ν_9, $\delta(C_\beta C_1)_{sym}$	257	264[d]		248

[a] This work. [b] Data from Takahashi et al.[38] [c] Data and assignment from Hu et al.[36] [d] Overlapping bands.

to its ferrous form and no denaturation of the protein. Upon addition of NO to NP1, significant differences are observed in

(37) Kitagawa, T. In *Biological Applications of Raman Spectroscopy*; Spiro, T. G., Ed.; Wiley-Interscience: New York, 1988; Vol. 3, pp 97−131.

(38) Takahashi, S.; Wang, J.; Rousseau, D. L. *Biochemistry* **1994**, *33*, 5531−5538.

(39) Hoshino, M.; Maeda, M.; Konishi, R.; Seki, H.; Ford, P. C. *J. Am. Chem. Soc.* **1996**, *118*, 5702−5707 and references therein.

Table 3. Resonance Raman High-Frequencies (cm^{-1}) of Nitrosyl and Cyano Adducts of NP1 at 298 K[a]

mode	NP1(NO)	NP1(CN^-)
ν_{10}	1636	1631
ν_2	1581	1581
ν_{37}	1562	1562
ν_{11}	1544	1544
ν_3	1504	1504
$\delta(C_bH_2)_{vinyl}$	1476	1468
ν_{28}	1427	1426
ν_{12}	1397	1402
ν_4	1375	1373

[a] See Table 1 for mode descriptions.

the frequencies and intensities of the structure-sensitive RR bands (Figure 1a−c, Tables 1 and 3). The band ν_4 shifts from 1372 to 1375 cm^{-1} and in the ν_3 region, the loss of the 1481-cm^{-1} band of the HS species and the observation of a band at 1504 cm^{-1} (Figure 1c) are characteristic of a 6cLS NO-ligated heme.[40−42] The ν_2 and ν_{10} modes of NP1 shift from 1560 and 1611 cm^{-1}, respectively, to 1581 and 1636 cm^{-1}, respectively, in NP1(NO). Significantly, the cyano complex of NP1, NP1(CN^-), has ν_2, ν_3, ν_4, and ν_{10} RR bands (Figure 1d) that are very similar to those of the nitrosyl complex (Table 3). These spectral behaviors further support a 6cLS ferric heme iron for the NO derivative of NP1, albeit the best answer as to the redox state of the RR sample must await a comparison of RR data for ferric− and ferrous−NO complexes of NP1.

The low-frequency (200−800 cm^{-1}) RR spectra of NP1(NO) in natural abundance and its ^{15}NO isotopically labeled analogue are shown in Figure 2 (traces b and c, respectively). Again, there is a distinct change in the spectral pattern upon binding of NO. In addition to the heme deformation modes, the low-frequency region contains modes associated with the bound exogenous ligand NO. The NP1(NO) spectrum exhibits a new band at 591 cm^{-1} (Figure 2b). The other difference is the appearance of an additional weaker feature at ∼578 cm^{-1}. $^{15}NO/^{14}NO$ substitution allows unambiguous identification of the Fe−NO vibrational modes, ν(Fe−NO) (stretching) and δ(Fe−N−O) (bending). The RR band at 591 cm^{-1} undergoes a 4-cm^{-1} downshift upon substitution of ^{14}NO with ^{15}NO (Figure 2c). A similar isotope shift has been observed for the ν(Fe−NO) vibration at 595 cm^{-1} in ferric metMb(NO).[42] Accordingly, the 591-cm^{-1} band in NP1(NO) is assigned to the ν(Fe−NO) stretching mode. The ∼578-cm^{-1} feature seems to disappear in the ^{15}NO adduct. It shifts most likely to ∼567 cm^{-1} overlapping with the protein band at ∼565 cm^{-1}, which results in a broader and more intense 566-cm^{-1} band (Figure 2c). Because of the large ∼11-cm^{-1} downshift, and by comparison with the δ(Fe−N−O) bending of metMb(NO) observed at 573 cm^{-1},[42] the ∼578-cm^{-1} band of NP1(NO) is assigned to the δ(Fe−N−O) vibration.

RR spectroscopy has proven to be an effective probe of the Fe−NO geometry in nitrosyl hemes and metalloporphyrins. In the absence of steric hindrance, the $Fe^{III}NO$ moiety is known to adopt a linear configuration normal to the heme plane on the basis of the total number of electrons in the metal d and ligand π^* orbitals, {FeNO}^{6}.[43] No bending mode of the Fe−N−O linkage has been observed for unhindered NO complexes of {FeNO}^{6} heme proteins.[29,44] Detection of the δ(Fe−N−O) mode in the NP1(NO) RR spectrum suggests some type of off-axis influence that induces a slightly distorted Fe^{III}−N−O configuration.[29,41] We carried out normal coordinate analysis (NCA) calculations based on the model (imidazole)−Fe(N_p)$_4$−N−O to verify the assignment of the observed ν(Fe−NO) and δ(Fe−N−O) RR bands and to examine the effect of the Fe−N−O angle on their vibrational frequencies. The results are summarized in Table 4. We found that the Fe−N−O angle value of 178° was best for reproducing the observed RR frequencies of NP1(NO) using physically reasonable force field constants. As shown in Table 4, the ^{15}NO isotopic shifts calculated for the stretching (591 cm^{-1}) and bending (578 cm^{-1}) Fe−NO modes agree well with the observed values. In the previous FTIR study of nitrosyl NP1, two ν(N−O) stretching absorption bands were reported at 1917 and 1904 cm^{-1}.[11] From the NCA calculations, it appears that the Fe−N−O angles of approximately 178° and 150° would give rise to such ν(N−O) frequencies, respectively (Table 4). However, no new bands corresponding to the calculated ν(Fe−NO) and δ(Fe−N−O) vibrational modes for a configuration with ∠(Fe−N−O) = 150° were discernible in the RR spectra of NP1(^{14}NO) and NP1(^{15}NO).

Table 4. Observed and Calculated Stretching (ν) and Bending (δ) Frequencies and Isotope Shifts (cm^{-1}) for the Fe−N−O Fragment of NP1(NO)[a]

observed		calculated		
mode	$\Delta(^{15}NO)$[b]	mode	$\Delta(^{15}NO)$[b]	PED[c] (%)
		∠(Fe−N−O) = 178.0°		
1917.0[d]	−37.5[d]	1917.1	−38.3	ν(NO)(93) + ν(FeNO)(9)
591.0	−4.0	591.0	−4.5	ν(FeNO)(80) + ν(NO)(7)
578.0	−11.0	578.0	−13.8	δ(FeNO)(90) + ν(FeNO)(6)
		∠(Fe−N−O) = 150.0°		
1904.0[d]	−37.0[d]	1902.7	−37.2	ν(NO)(95) + ν(FeNO)(7)
		698.5	−14.7	ν(FeNO)(65) + δ(FeNO)(30)
		485.2	−5.0	δ(FeNO)(60) + ν(FeNO)(20)

[a] Force constants used: K(ImFe) = 1.4500, K(FeN) = 4.0900, K(NO) = 15.1100, K(FeN$_p$) = 1.0000, H(ImFeN) = 0.3500, H(FeNO) = 0.8712, F(FeN/NO) = 0.2000, F(ImFe/NO) = 0.2500, F(FeN/FeNO) = 0.0790. The units are mdyne $Å^{-1}$ for K (stretching) and F (interaction) force constants, and mdyne Å rad^{-2} for H (bending) force constants. [b] Observed or calculated shifts upon ^{15}NO substitution. [c] Calculated potential energy distribution (%) with respect to force constants for natural abundance molecule. [d] Data from FTIR measurements by Ding et al.[11]

As discussed in the Introduction, the crystal structure of NP1($Fe^{III}NO$) is not known, but the crystal structure of the highly homologous complex NP4($Fe^{III}NO$) has very recently been determined and found to have an Fe−N−O angle equal to 156°.[16] The reason for the discrepancy between the NP1 RR and the NP4 X-ray results is not yet clear, but is likely related to one of the following four factors. First, it is possible that, despite the overall similarity between NP1 and NP4, they do in fact bind NO with differing geometries. Alternatively, it is possible that the RR bands corresponding to the bent NO conformer are buried under those derived from the strong heme modes. A third possibility is that there is a fundamental difference between the solution and crystalline Fe−NO configurations. Or, fourth, perhaps the modeling based on an undistorted heme coordination geometry is insufficient to capture the vibrational character of the nitrosyl complex in the nitrophorins, where the heme is highly ruffled. Indeed, a correlation

(40) Yu, N. T.; Kerr, E. A. In *Biological Applications of Raman Spectroscopy*; Spiro, T. G., Ed.; Wiley-Interscience: New York, 1988; Vol. 3, pp 39−95.
(41) Hu, S.; Kincaid, J. R. *J. Biol. Chem.* **1993**, *268*, 6189−6193.
(42) Benko, B.; Yu, N.-T. *Proc. Natl. Sci. U.S.A* **1983**, *880*, 7042−7046.
(43) Feltham, R. D.; Enemark, J. H. *Coord. Chem. Rev.* **1974**, *13*, 339−406.
(44) Yu, N. T.; Lin, S. H.; Chang, C. K.; Gersonde, K. *Biophys. J.* **1989**, *55*, 1137−1144.

between ruffled hemes and bent nitrosyl and cyano geometries has been noted.[16]

The ν(Fe−NO) frequency at 591 cm^{-1} in NP1(NO) is typical of a ferric 6cLS NO complex, indicating typical Fe^{III}−NO bond strength, and is located 4 cm^{-1} lower than that of ferric metMb-(NO), whereas the δ(Fe−N−O) frequency at 578 cm^{-1} is higher by 5 cm^{-1}. That the NP1 Fe^{III}−NO bond is typical indicates that the structural basis for the tighter NO binding in NP1 relative to metMb[10] is not linked to a stronger iron−nitrosyl bond. NCA calculations indicate that the magnitude of separation between the stretching and bending modes frequencies becomes larger as the Fe−N−O angle decreases (Table 4). This is consistent with a slightly less distorted Fe−N−O linkage occurring in NP1 than in metMb, with a correspondingly smaller frequency separation between the ν(Fe−NO) and δ(Fe−N−O) modes and a smaller isotope shift for the ν(Fe−NO) mode. Regardless, theoretical studies[45] support the hypothesis that the Fe−N−O in-plane bending mode is especially low in energy.

Kinetic binding rates and the Soret absorption maximum of nitrophorins are pH dependent: at pH 7.0, the NO-bound protein is less stable and the ligand is displaced if the protein is diluted or exposed to an argon atmosphere, whereas at pH 5.0, release of NO is hindered, possibly due to a change in the protein dynamics.[10] The pH dependence appears to be due to a single ionizable group with a pK_a of about 6.5.[9,10] To determine any structural difference in the heme conformation of NP1 with respect to pH that might influence NO binding, we measured RR spectra of NP1 and its NO adduct at pH 5.0 and 7.0. However, interestingly, no differences between pH 5.0 and 7.0 were observed in either the high- or low-frequency regions, including the ν(Fe−NO) frequency region, which suggests that no conformational change of the heme group occurred during the pH transition, even in the presence of exogenous ligand. These RR results reveal that the group affecting the rate of NO release is not directly bound to the heme, and completely rule out the possibility of loss of the proximal histidine ligand at pH 5.0, which had been suggested by recent calculations.[46] Consistent with this, the NP4(NO) crystal structures at pH 5.6 and 7.0 display the same closed conformer.

Cyanide Binding to NP1. Band positions for heme structure-sensitive modes in the RR spectrum of the cyano complex of NP1 (Figure 1d, Table 3) are consistent with a 6cLS heme iron. The X-ray crystal structure of cyano NP1, NP1(CN$^-$), shows the heme conformation as more ruffled than that of cyano metMb, metMb(CN$^-$).[13] Distorted porphyrins are known to exhibit lower frequencies for the RR structure-sensitive marker lines.[47,48] Ma et al.[49] recently investigated the conformational differences in the hemes of ferricytochromes c_3 by RR spectroscopy, molecular mechanics calculations, and normal coordinate structural decomposition, and showed that the heme ring modes ν_3 and ν_{10} are useful indicators of the nonplanar distortions in cytochromes c_3. It also appeared from their study that ν_{10} exhibits a larger sensitivity to porphyrin nonplanarity than ν_3 and that ruffling is the dominant factor influencing the RR frequencies. The ν_{10} mode occurs at 1631 and 1641 cm^{-1} for NP1(CN$^-$) (Figure 1d) and metMb(CN$^-$),[50] respectively, which is consistent with a more ruffled heme in NP1(CN$^-$). In cytochromes c_3, the ν_3 frequencies were deconvoluted at 1501, 1497, 1507, and 1502 cm^{-1} for hemes 1−4, respectively, while the ν_{10} frequencies were deconvoluted at 1633, 1626, 1638, and 1634 cm^{-1} for hemes 1−4, respectively.[49] By comparison to the cytochromes, the ν_3 and ν_{10} frequencies of NP1(CN$^-$) at 1504 and 1631 cm^{-1}, respectively, predict that the heme macrocycle of cyano NP1 is ruffled to a degree similar to that of cytochromes c_3 (∼0.8 Å). Interestingly, the ultrahigh-resolution structures of NP4(CN$^-$) and NP4(NO) display hemes ruffled to ∼0.8 Å.[16] The comparison of the heme structure-sensitive modes between the NP1(NO) and NP1(CN$^-$) complexes (Table 3) also suggests a somewhat smaller distortion from planarity in nitrosyl NP1 relative to cyano NP1.

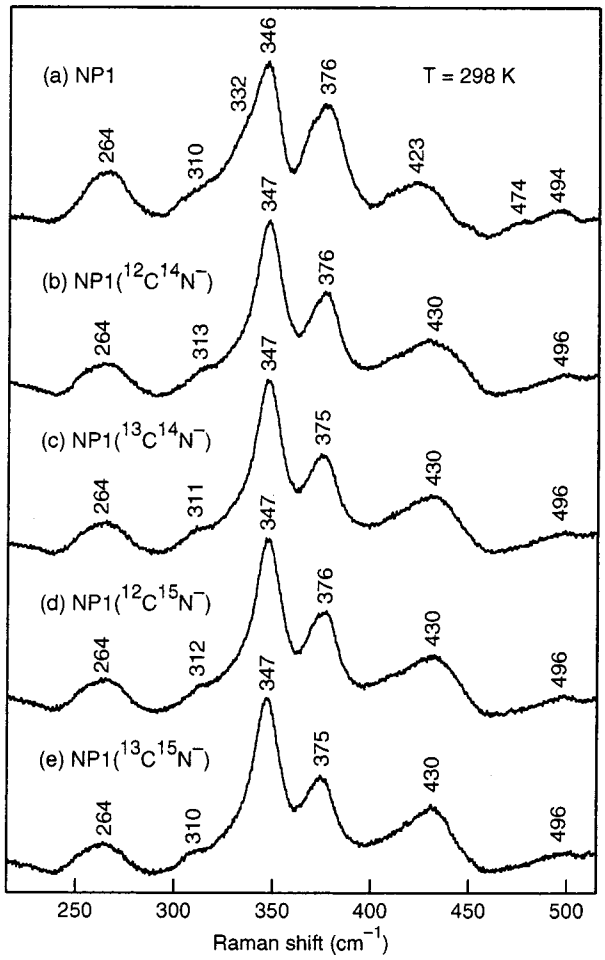

Figure 3. Low-frequency (215−515 cm^{-1}) RR spectra of (a) NP1 and (b−e) its $^{12}C^{14}N$, $^{13}C^{14}N$, $^{12}C^{15}N$, and $^{13}C^{15}N$ adducts obtained from spinning NMR tubes at room temperature: 413.1-nm excitation, 70-mW laser power, and 6-cm^{-1} slit widths.

Figure 3 shows the RR spectra in the 215−515-cm^{-1} region of NP1 and its $^{12}C^{14}N^-$, $^{13}C^{14}N^-$, $^{12}C^{15}N^-$, and $^{13}C^{15}N^-$ adducts obtained at 298 K with Soret-band excitation (413.1 nm). Because a number of strong heme deformation vibrational modes occur in this frequency region, the modes associated with the Fe^{III}−CN$^-$ bond are not readily noticeable in the room-temperature spectra. However, contributions from the CN-isotope dependent modes become evident in the difference spectra plotted in Figure 4, where several bands in the 300−

(45) Vangberg, T.; Bocian, D. F.; Ghosh, A. *J. Biol. Inorg. Chem.* **1997**, *2*, 526−530.
(46) Gérczei, T.; Fazekas, Á.; Keserú, G. M. *J. Mol. Struct.* **2000**, *503*, 51−58.
(47) Shelnutt, J. A.; Medforth, C. J.; Berber, M. D.; Barkigia, K. M.; Smith, K. M. *J. Am. Chem. Soc.* **1991**, *111*, 4077−4087.
(48) Jentzen, W.; Simpson, M. C.; Hobbs, J. D.; Song, X. Z.; Ema, T.; Nelson, N. Y.; Medforth, C. J.; Smith, K. M.; Veyrat, M.; Mazzanti, M.; Ramasseul, R.; Marchon, J. C.; Takeushi, T.; Goddard, W. A., III; Shelnutt, J. A. *J. Am. Chem. Soc.* **1995**, *117*, 11085−11097.
(49) Ma, J.-G.; Zhang, J.; Franco, R.; Jia, S.-L.; Moura, I.; Moura, J. J. G.; Kroneck, P. M. H.; Shelnutt, J. A. *Biochemistry* **1998**, *37*, 12431−12442.
(50) Hirota, S.; Ogura, T.; Shinzawa-Itoh, K.; Yoshikawa, S.; Kitagawa, T. *J. Phys. Chem.* **1996**, *100*, 15274−15279.

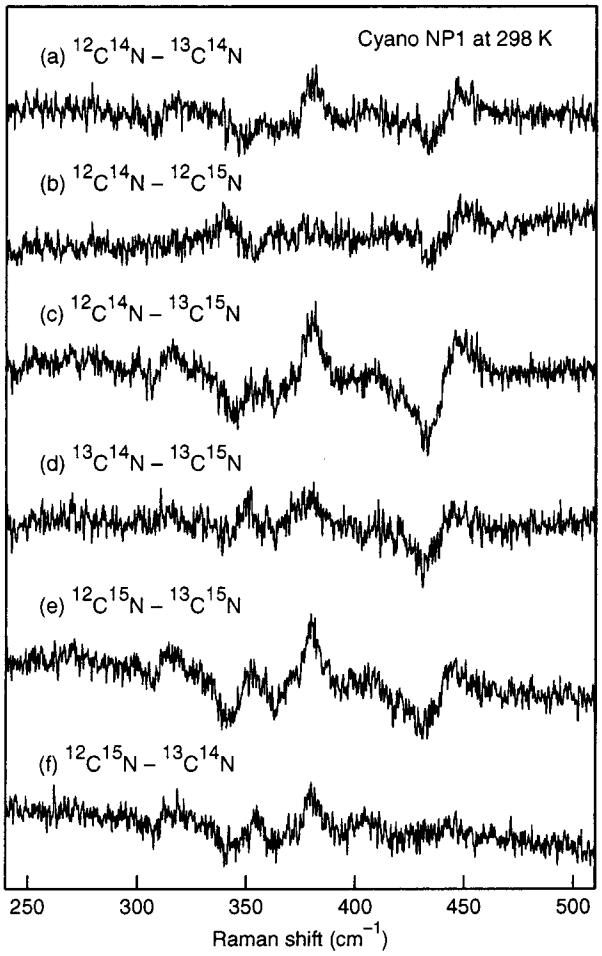

Figure 4. CN isotope difference spectra in the 240−510 cm^{-1} range for NP1(CN$^-$) at 298 K generated by the digital subtraction of the various spectra shown in Figure 3.

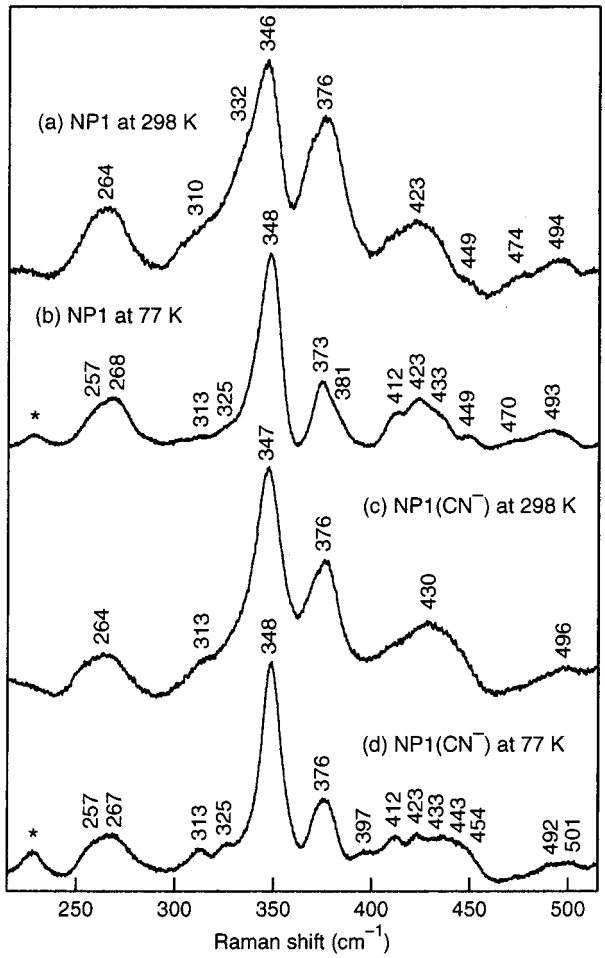

Figure 5. Low-frequency (215−515 cm^{-1}) RR spectra of (a, b) NP1 and (c, d) NP1(CN$^-$) obtained at (a, c) 298 and (b, d) 77 K. Spectra were run as described in Figure 1 with 413.1-nm excitation: 70-mW (298 K), 150-mW (77 K), and 6-cm^{-1} slit widths.

465-cm^{-1} region do not completely cancel in all the difference spectra (a−f). Moreover, as shown in Figures 5 (absolute spectra) and 6 (difference spectra), spectral resolution is considerably improved at 77 K, which allows clear observation of vibrational modes that are sensitive to isotope labeling of the cyano group. To identify these modes, we carried out curve-fitting analyses in which individual bands were assumed to be Gaussian, and their positions, peak intensities, and widths were adjusted to reproduce the observed raw and difference spectra. The final deconvoluted spectra for frozen four NP1(CN$^-$) isotopomers are depicted in Figure 7 and the peak positions estimated from the fitting procedure are summarized in Table 5. As shown in Table 5, at least 10 cyanide isotope-sensitive modes are uncovered in the vibrational frequency range of 250−460 cm^{-1}.

In most cyano heme proteins, the Fe^{III}−CN$^-$ coordination group adopts a linear structure, giving rise to the observation of only a stretching Fe−cyanide mode, ν(Fe−CN), in the Soret excitation RR spectra. However, the bending Fe−cyanide mode, δ(Fe−C−N), can be activated by slight distortions of the "essentially linear" Fe−C−N linkage by steric or electronic factors and the identity of the two modes can be established by their characteristic vibrational frequencies and cyanide−isotope dependence.[22,31] In a linear Fe−C−N oscillator, the ν(Fe−CN) mode tends to vibrate at higher frequency than the δ(Fe−C−N) mode and shifts monotonically with an increase of the total mass of the cyanide isotopomer, whereas the lower frequency δ(Fe−C−N) exhibits a "zigzag" pattern isotope dependence (decrease−increase−decrease).[22] The appearance of a new band at 454 cm^{-1} in the RR spectrum of NP1(CN$^-$) that exhibits a monotonic isotope shift pattern as the mass of cyanide increases from $^{12}C^{14}N$ to $^{13}C^{15}N$ (Figure 7a−d) corresponds to the ν(Fe−CN) stretching vibration (Table 5). Another cyanide isotope-sensitive band for NP1(CN$^-$) can be seen at 397 cm^{-1} (Figure 7a, Table 5). This band is absent in the RR spectrum of NP1 (Figure 5c) and shows a zigzag pattern isotope dependence. Accordingly, we assign the band at 397 cm^{-1} to the δ(Fe−C−N) bending vibration of NP1(CN$^-$) in which the Fe−C−N moiety assumes a linear conformation. In Figure 7, the observation of an additional Fe−CN vibration at 443 cm^{-1} with a zigzag pattern (Table 5) suggests the presence of a different cyano NP1 population. The existence of a fourth Fe−CN mode is less apparent in both the absolute and the difference spectra. However, careful deconvolution of the RR spectra of NP1(CN$^-$) isotopomers reveals the presence of an overlapping band at 357 cm^{-1} for NP1($^{12}C^{14}N^-$) (Figure 7a), which is absent in the spectrum of NP1 (Figure 5b) and exhibits a small zigzag frequency shift upon substitution with isotopically labeled cyanides (Figure 7b−d, Table 5). This spectral behavior of the 443- and 357-cm^{-1} bands assigns these bands to heavily coupled ν(Fe−CN) and δ(Fe−C−N) vibrations, characteristic of a bent bonding configuration of the Fe−C−N group. Other RR bands at 257, 267, 313, 326, 379, 433, and 449 cm^{-1} exhibit cyanide isotope dependence as well. The frequencies of these vibrations coincide with those seen for NP1 (Table 5) and the observed

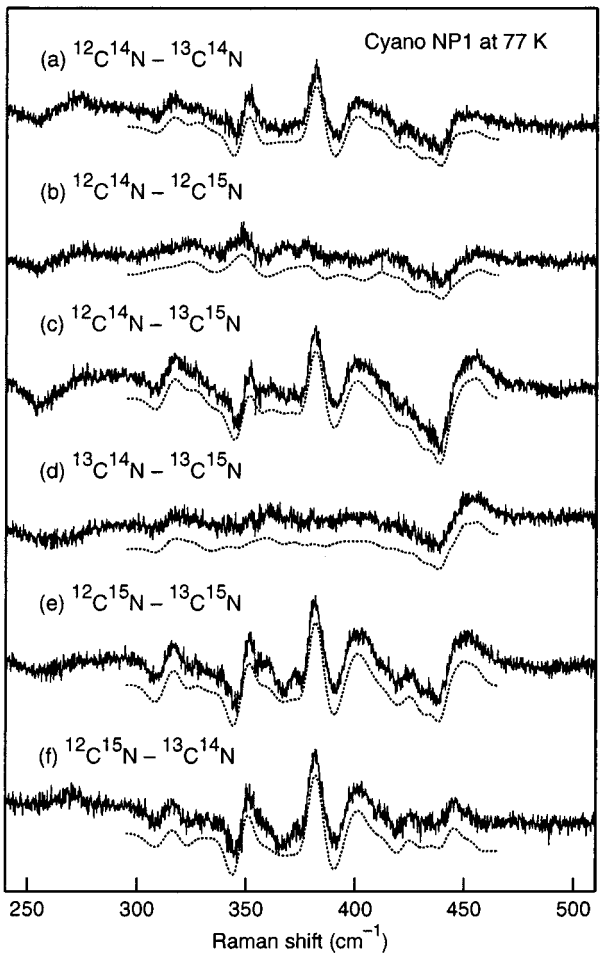

Figure 6. CN isotope difference spectra for NP1(CN^-) at 77 K generated by the digital subtraction of the various spectra shown in Figure 7: solid lines, observed in the 240−510 cm^{-1} region; dotted lines, curve fitted in the 295−465 cm^{-1} region.

Table 5. Resonance Raman Frequencies (cm^{-1}) for NP1 and Cyano Adducts of NP1 at 77 K Obtained by Curve Fitting Analysis

NP1	$^{12}C^{14}N$	$^{13}C^{14}N$	$^{12}C^{15}N$	$^{13}C^{15}N$
	454.4	453.0	452.6	451.4
449.3	449.4	448.1	448.0	446.5
	442.8	440.4	441.0	439.6
433.1	432.5	432.4	432.2	432.2
422.8	423.2	423.2	423.4	423.5
411.9	412.1	411.9	412.2	412.2
	396.8	392.0	396.8	391.6
380.6	379.0	377.4	379.0	377.3
373.1	372.0	372.0	372.0	371.7
	356.6	355.6	356.6	355.6
348.7	348.6	348.2	348.6	348.2
340.5	340.5	340.5	340.4	340.2
325.5	325.5	324.9	325.5	325.1
312.6	312.6	311.3	312.5	310.8
276.8	277.2	277.2	277.2	277.2
268.2	267.3	266.6	267.1	266.6
256.9	256.6	255.9	256.2	255.8

isotope shifts are assumed to arise from their kinematic coupling to the Fe−CN vibrations. A similar effect of cyanide isotope substitution was recently found by Hirota et al. for the low-frequency RR heme bands of cyano metMb and cyano metHb.[50]

To assign the four RR features associated with the cyanide ligand of NP1, NCA calculations were carried out based on the (imidazole)−Fe(N_p)$_4$−C−N models with varying Fe−C−N and N_p−Fe−C angles. The frequencies and potential energy distribution (PED) are presented in Table 6. For the first set of Fe−CN vibrational modes (454 and 397 cm^{-1}), the angles ∠(Fe−C−N) = 173° and ∠(N_p−Fe−C) = 90° were chosen based on the X-ray crystal structure data and that essentially linear cyano complexes tend to produce stretching modes at higher frequencies than the bending modes. The NCA analysis revealed that the experimental RR data for NP1($^{12}C^{14}N^-$) can be fit with a physically reasonable force field (Table 6). However, the observed frequencies for the other cyanide isotopomers could not be effectively reproduced by calculations. The observed isotope shifts are all smaller than those predicted for a vibrationally isolated linear Fe−C−N group. This discrepancy is attributed to the existence of strong coupling interactions between Fe−CN and heme vibrational modes, as revealed by the effect of cyanide isotope substitution on a number of heme RR bands (Table 5). When tilting of the Fe−C−N linkage was considered by allowing the N_p−Fe−C angles to deviate from

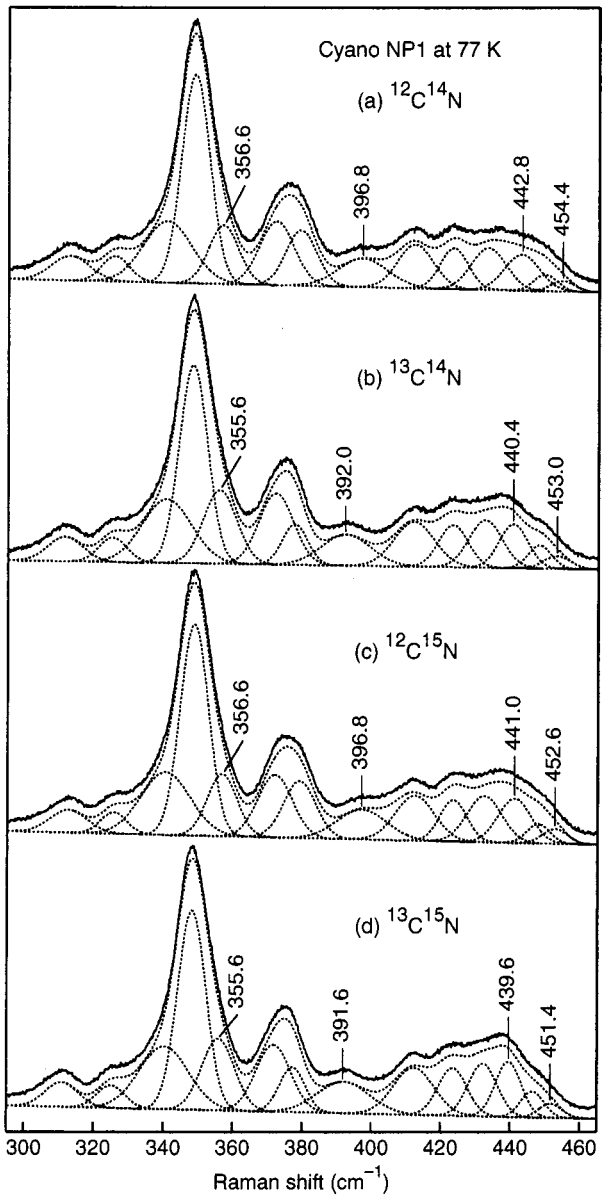

Figure 7. Low-temperature (77 K) RR spectra and curve-fitting analyses of the indicated cyano NP1 in the 295−465 cm^{-1} region. Spectra were run as described in Figure 1 with 413.1-nm excitation (150 mW) and 6-cm^{-1} slit widths. Vibrational frequencies of the deconvoluted bands are given in Table 5. Predominantly Fe−CN bands are correlated.

Table 6. Observed and Calculated Stretching (ν) and Bending (δ) Frequencies and Isotope Shifts (cm^{-1}) for the Fe−C−N Fragment of NP1(CN^-)[a]

observed mode($\Delta^{13}C$, ^{15}N, $^{13}C^{15}N$)[b]	calculated mode($\Delta^{13}C$, ^{15}N, $^{13}C^{15}N$)[b]	calculated PED (%)[c]
	∠(Fe−C−N) = 172.9°	
2135.0 (−, −, −)[d]	2135.4 (45.9, 31.3, 78.0)	ν(CN)(99)
454.4 (1.4, 1.8, 3.0)	454.5 (4.2, 4.6, 8.5)	ν(FeCN)(84) + ν(FeIm)(14)
396.8 (4.8, 0.0, 5.2)	396.8 (9.8, 2.0, 11.9)	δ(FeCN)(75) + δ(ImFeC)(16)
	∠(Fe−C−N) = 155.0°	
2124.0 (−, −, −)[d]	2125.8 (45.0, 31.8, 77.6)	ν(CN)(100)
442.8 (2.4, 1.8, 3.2)	442.7 (8.4, 2.3, 10.7)	ν(FeCN)(75) + δ(FeCN)(19) + ν(FeIm)(11)
356.6 (1.0, 0.0, 1.2)	356.5 (4.5, 2.3, 6.6)	δ(FeCN)(46) + δ(ImFeC)(16) + ν(FeIm)(11)

[a] Force constants used: for Fe−C−N angle = 172.9°, K(ImFe) = 1.4500, K(FeC) = 1.9790, K(CN) = 17.1520, K(FeN_p) = 1.0000, H(ImFeC) = 0.4500, H(FeCN) = 0.3495, F(FeC/CN) = 0.3400, F(ImFe/CN) = 0.2180, F(FeC/FeCN) = 0.0790; for Fe−C−N angle = 155.0° same as for Fe−C−N angle = 172.9° with the exception of K(FeC) = 1.5510, and H(FeCN) = 0.3140. The units are mdyn $Å^{-1}$ for K (stretching) and F (interaction) force constants, and mdyn Å rad^{-2} for H (bending) force constants. [b] Numbers in parentheses are observed or calculated shifts upon ^{13}C, ^{15}N, and $^{13}C^{15}N$ substitution for the CN atoms. [c] Calculated potential energy distribution (%) with respect to force constants for natural abundance molecule. [d] Infrared absorption bands; isotopic data not available.

90°, only small changes in the calculated ν(Fe−CN) and δ(Fe−C−N) frequencies (less than 3 cm^{-1}) and isotope shifts (less than 1 cm^{-1}) were obtained (data not shown), and the exact orientation of the cyanide ligand in the linear form could not be determined from the 454 and 397 cm^{-1} vibrational modes. In fitting the frequencies of the second set of Fe−CN vibrations (443 and 357 cm^{-1}), only the Fe−C−N angle and the force constants for the Fe−C and Fe−C−N coordinates were allowed to vary (Table 6). When permitting this, the calculations gave rise to a "bent" model (Fe−C−N angle of 155°) with somewhat lowered force constants. As has already been shown for cyano complexes of heme proteins,[30,31,51,52] the separation between the two Fe−CN modes, ν(Fe−CN) and δ(Fe−C−N), is increased in the bent form compared to the linear form (86 versus 57 cm^{-1}). Although observed and calculated cyanide isotope shifts again show discrepancies, the zigzag isotope shifting pattern detected for the 443- and 357-cm^{-1} modes is reproduced by the calculations using the bent Fe−C−N model. It is known that when the Fe−CN fragment adopts a bent structure, the ν(Fe−CN) and δ(Fe−C−N) modes are vibrationally mixed with each other and both exhibit partially zigzagged patterns depending on the extent of mixing.[31] Further evidence for two different cyano NP1 populations was obtained from FTIR measurements (spectra not shown), which revealed two ν(C≡N) absorption bands at 2135 and 2124 cm^{-1}, the frequencies calculated in the NCA at 2135 and 2126 cm^{-1} for the linear and bent configurations, respectively (Table 6).

The ν(Fe−CN) mode of metMb(CN^-) was observed around 452 cm^{-1} and no δ(Fe−C−N) RR band was detected.[50] Another isotope-sensitive band at 441 cm^{-1} with a zigzag pattern was found and it was suggested to arise from a coexisting bent structure as a minor population.[50] The absence of bending modes for metMb(CN^-) suggests that the Fe−C−N linkage geometry is much more fixed in cyano metMb than in cyano NP1.

Concluding Remarks

In summary, the RR data reveal the Fe^{III}−O bond strength in NP1 to be typical for ferric nitrosyl heme proteins. Furthermore, the heme proximal ligand, His 59, remains ligated to the {FeNO}^{6} center in solution over the entire pH range investigated (5.0−8.0), in agreement with the available electrochemical data for NP1[10] and crystallographic data for NP4.[15] The RR data also show that the linear Fe^{III}−CN^- bond can be distorted in NP1. In the absence of direct hydrogen bonding to the cyano moiety, as found in the NP1(CN^-) crystal structure,[13] it is possible that unfavorable electrostatic interactions between Asp 30 and CN^-, or electronic effects on ligating with the ruffled heme, are responsible for generating the bent configuration.

Acknowledgment. This work was supported by grants from the Robert A. Welch Foundation (E-1184 to R.S.C.), National Institute of General Medical Sciences (GM-48370 to R.S.C.), and National Institutes of Health (HL-54826 to F.A.W. and HL-62969 to W.R.M.). The authors thank Ms. Celia Balfour for preparation of the pure recombinant NP1 protein and Dr. Patrick Killough (Shell Development Co.) for measuring the aqueous FTIR spectrum of NP1(CN^-).

JA0031927

(51) Al-Mustafa, J.; Kincaid, J. R. *Biochemistry* **1994**, *33*, 2191−2197.
(52) Al-Mustafa, J.; Sykora, M.; Kincaid, J. R. *J. Biol. Chem.* **1995**, *270*, 10449−10460.